Magnetization reversal times in the two-dimensional Ising model

Kevin Brendel, G. T. Barkema, and Henk van Beijeren
Theoretical Physics, Utrecht University, Leuvenlaan 4, 3584 CE Utrecht, The Netherlands
(Received 17 October 2002; published 26 February 2003)

We present a theoretical framework which is generally applicable to the study of time scales of activated processes in systems with Brownian type dynamics. This framework is applied to a prototype system: magnetization reversal times in the two-dimensional Ising model. Direct simulation results for the magnetization reversal times, spanning more than five orders of magnitude, are compared with theoretical predictions; the two agree in most cases within 20%.

DOI: 10.1103/PhysRevE.67.026119 PACS number(s): 02.50.Ey, 05.10.Gg, 05.40.Fb, 05.40.Jc

I. INTRODUCTION

Activated processes that can be described with some type of Brownian dynamics are abundant in the world around us. Well-known examples are the nucleation of droplets in an undercooled gas or of crystals in an undercooled liquid, chemical reactions and the escape of a protein from a misfolded state. A prototype system to study such phenomena numerically is the well-known Ising model. Above the so-called critical temperature, in absence of an external magnetic field, up- and down-pointing spins are roughly equally abundant. Below the critical temperature, the system prefers to be in either of two states: one state with a positive magnetization in which most spins are pointing up, and one state with a negative magnetization. As long as the system size remains finite, reversals of the magnetization—transitions between positive and negative magnetization—are possible and will occur at a certain average frequency. These processes are activated, since configurations with magnetization close to zero have a higher free energy than typical configurations with a magnetization close to either of the equilibrium values.

In this manuscript, we study the time scales associated with magnetization reversal. A theoretical framework is outlined which is generally applicable to activated processes in systems with Brownian type dynamics, and compared to high-accuracy computer simulations. From a practical point of view magnetization reversals are also of great interest because of applications in memory devices and the like. One wants to have rapid switching of magnetization under reversals of an external field, but no spontaneous reversals of the magnetization, even if the external field has been turned off. In the literature much attention has been paid to reversal time distributions in the presence of a driving field [1,2]. In the fieldless case, much work has been done exactly at the critical temperature, see for instance Ref. [3]. Here, large-scale fluctuations in the magnetization decay at a time proportional to L^z, where z is the dynamical critical exponent. However, spontaneous reversals below the critical temperature in the absence of a field have hardly been studied. Here we consider the latter case for the prototypical case of an Ising model with periodic boundary conditions. We identify the leading scenario for reversals of the magnetization and show that the process may be described to a good approximation by a one-dimensional diffusion process over a potential barrier.

Our manuscript is organized as follows. In Sec. II, we describe the model that we study in detail. In Sec. III, we outline the theoretical framework which is generally applicable to activated processes in systems with Brownian type dynamics. We then apply this framework to our prototypical model—magnetization reversal in the Ising model. In Sec. IV we compare the theoretical predictions with high-accuracy computational results.

II. DETAILED DESCRIPTION OF THE MODEL

We consider the Ising model on a $B\times L$ rectangular lattice with periodic (helical) boundary conditions, with the Hamiltonian

$$H=-J\sum_{\langle i,j\rangle}\sigma_i\sigma_j, \tag{1}$$

in which $\sigma_i=\pm 1$ is the spin at site i and J is the coupling constant. The summation runs over all pairs of nearest-neighbor sites; those of site i are $j=i\pm 1$ modulo N and $j=i\pm B$ modulo N, with $N=BL$. The magnetization is defined as $M\equiv\Sigma_i\sigma_i$; it can take values $M=-N,-N+2,\ldots,N$; all through this manuscript, we restrict ourselves to systems in which both B and L are even. As a consequence, M takes only even values, and summations over a range of possible magnetizations only run over even numbers, with an increment of 2.

A well-known property of the model is that at sufficiently low temperatures, the distribution of the magnetization $M\equiv\Sigma_i\sigma_i$ becomes bimodal—the spins in a configuration tend to align around the two preferred values $\pm M_0$. For infinite systems this occurs at all temperatures below the critical temperature $T_c=J/(0.440\,69k_B)$, for finite systems this range starts at slightly different temperatures.

The system evolves in time according to single-spin-flip dynamics with Metropolis acceptance probabilities [4,5]. If C_i is the configuration after i proposed spin flips, a trial configuration C'_{i+1} is generated by flipping a single spin at a random site. This trial configuration is then either accepted ($C_{i+1}=C'_{i+1}$) or rejected ($C_{i+1}=C_i$); the acceptance probability is given by

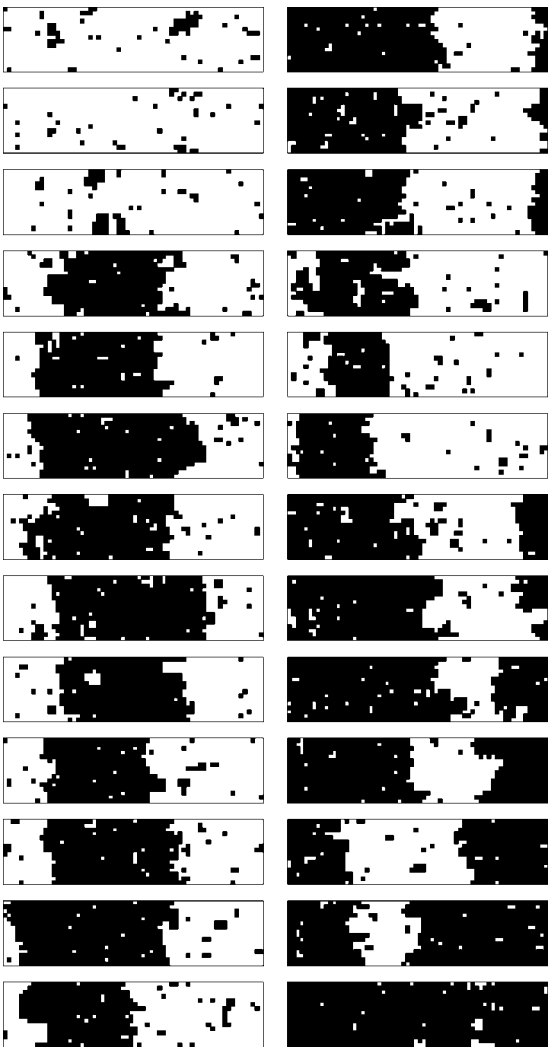

FIG. 1. Snapshots of the transition from a state with most spins down to a state with most spins up in the 16×64 Ising model, taken at equal time intervals of 500 attempted spin flips per site, at inverse temperature $\beta J=0.5$.

$$P_a=\min[1,\exp[-\beta(E(C'_{i+1})-E(C_i))]], \tag{2}$$

in which $\beta=1/(k_BT)$ with Boltzmann constant k_B and temperature T. The time scale is set such that in one unit of time, on average each spin is proposed to be flipped once. So in our system, in one unit of time we perform BL Monte Carlo steps.

Our current interest in the Ising model with single-spin-flip dynamics stems from the fact that in finite systems, the configurations will occasionally switch between states in which the magnetization is either negative or positive, through an activated process. The dominant pathway at low temperatures consists of the formation of a single pair of closed interfaces in the shorter periodic direction (for $B\neq L$), which perform a relative diffusive motion around the longer periodic direction and annihilate after meeting each other through the periodic boundary. A series of snapshots, illustrating this process, is presented in Fig. 1.

III. THEORETICAL FRAMEWORK

To study the behavior of times between magnetization reversals at temperatures below the critical one we may consider an ensemble of a large number of systems prepared in states with a magnetization close to the equilibrium value $-M_0$ and study the rate at which these systems reach the value $M=M_0$, after which they are removed from the ensemble. Alternatively, the behavior of times between zero crossings of the magnetization can be studied, as discussed below. The spin-flip dynamics described above may be represented by a master equation for the probability distribution $P(\boldsymbol{\sigma})$ of finding a system in the state $\boldsymbol{\sigma}$ at time t. Due to the huge number of possible states this master equation cannot be solved analytically or even numerically for system sizes of practical interest. Therefore, as an approximation we assume that we may replace the exact master equation by an approximate master equation for the probability $P(M,t)$ of finding a system with magnetization M at time t. The form of this equation is

$$\frac{dP(M,t)}{dt}=\Gamma_{M,M+2}P(M+2,t)+\Gamma_{M,M-2}P(M-2,t) -(\Gamma_{M+2,M}+\Gamma_{M-2,M})P(M,t) \tag{3}$$

with $\Gamma_{M',M}$ the transition rate from M to M'. It ignores the fact that the actual transition rates will depend on the geometry of the state under consideration, with the idea that in typical cases spin states of very similar geometry will dominate the set of states with given M. Besides on M and β the transition rates will depend on the geometry of the system, that is on B and L. To estimate the scaling behavior of these dependencies we make two further simplifying assumptions as follows.

(i) First of all, requiring $B\leqslant L$, we assume that states with $M\neq\pm M_0$ consist of a single strip of opposite magnetization separated by two phase boundaries of length B from the majority spin phase. The relevant changes of M then will be caused by displacements of these boundaries due to flips of spins along them. The total number of spins available for this will be proportional to B, hence the transition rates should also be proportional to B and independent of L.

This approximation will not be valid for values of M that are too close to $\pm M_0$, as for these the opposite magnetization will typically be found in a closed cluster rather than in a strip. It will turn out though that the contributions from these M values to the reversal frequency are very small for systems of reasonable length. Therefore, using the approximation $\Gamma\sim B$ also here does not harm. Further we neglect the possibility of having more than one strip of opposite magnetization. When the temperature gets close to the critical one, when B becomes small or when L becomes very large, this may not be a good approximation. We will come back to this in Sec. V. In our further theoretical treatment we will assume that we are in a situation where the single-strip approximation is justified.

(ii) Further we neglect changes due to fluctuations of the magnetization caused by the growth and shrinkage of small clusters of the minority spin type. On average these do not

contribute to magnetization reversals, so this approximation should be allowed. In case one considers the first passage frequency through zero magnetization there is a small effect, to which we will come back in Sec. V too.

In order that the equilibrium distribution be a stationary solution of the master equation we impose the condition of detailed balance

$$\frac{\Gamma_{M,M+2}}{\Gamma_{M+2,M}} = \exp[\beta(F(M) - F(M+2))], \tag{4}$$

where $\beta F(M) = -\ln P_{eq}(M)$, with $P_{eq}(M)$ the equilibrium probability of magnetization M. In Sec. IV B it will be explained how this condition may be combined with simulation results for interface diffusion to obtain approximations for all transition rates that lead to a good overall prediction of the reversal times.

The long-time reversal frequency as predicted by master equation (3) follows as the largest eigenvalue of this equation, supplemented with an absorbing boundary at $M=A$, with either $A=M_0$ or $A=0$. The first choice corresponds to a real reversal of the magnetization, the second one to a first return to the value $M=0$. After this the system will have equal probabilities to actually reverse its magnetization or to return to the equilibrium magnetization value it came from, hence this return frequency should be twice the reversal frequency. The absorbing boundary condition is implemented by setting $\Gamma_{A-2,A}$ equal to zero.

The largest eigenvalue $-\nu$ of $\Gamma_{M,M'}$ in Eq. (3), as well as the corresponding eigenvector $P_0(M)$, may be found by requiring that the net current away from magnetization M assumes the value $\nu P_0(M)$. Using conservation of probability one easily checks that this may be expressed as

$$\Gamma_{M+2,M} P_0(M) - \Gamma_{M,M+2} P_0(M+2) = \nu \sum_{m \leqslant M} P_0(m), \tag{5}$$

$$\nu = \frac{\Gamma_{A,A-2} P_0(A-2)}{\sum_{m \leqslant A-2} P_0(m)}. \tag{6}$$

In Eq. (5) $P_0(m)$ on the right-hand side may be approximated, up to a normalization factor, by $\exp[-\beta F(m)]$, because the sum is dominated by the terms with small m values, for which this approximation is excellent. This one may check in hindsight against the solution obtained. With this approximation the equation may be solved recursively for $P_0(M)$ in terms of $P_0(A-2)$ for $M=A-4,A-6$, etc. with the result

$$P_0(M) = \sum_{M \leqslant m \leqslant A-2} \frac{\Gamma_{A,A-2}}{\Gamma_{m+2,m}} \exp[\beta(F(m) - F(M))] \times \frac{\sum_{n \leqslant m} \exp[-\beta F(n)]}{\sum_{n' \leqslant A-2} \exp[-\beta F(n')]} P_0(A-2). \tag{7}$$

The summations over m and M are dominated by values of m close to zero, combined with values for M close to $-M_0$, for which the sum over n is basically independent of m. Therefore, the reversal frequency may be obtained as

$$\nu = \frac{\Gamma_{A,A-2} P_0(A-2)}{\sum_{M \leqslant A-2} P_0(M)} = \left(\sum_{m=-M_0}^{A-2} \frac{\exp[\beta F(m)]}{\Gamma_{m+2,m}} \sum_{n \leqslant A-2} \exp[-\beta F(n)] \right)^{-1}. \tag{8}$$

The restriction of the summation over m to values $m > -M_0$ is needed to avoid large spurious contributions from $m < -M_0$. The result in Eq. (8) is well-known. It is usually derived by considering a state with a stationary current in which mass is inserted at a constant rate on one side (e.g., at $M=-B\times L$ in our case) and taken out as soon as it reaches the absorbing boundary (see, e.g., Ref. [6], Sec. IV E). In that case the replacement of the sum over n by a constant is exact.

IV. SIMULATIONS AND RESULTS

In order to apply the above theoretical framework to magnetization reversal times in the Ising model, the two ingredients required are: (i) the equilibrium probability $P_{eq}(M)$ to find the system in a state with magnetization M and (ii) the transition rates $\Gamma_{M',M}$ from magnetization M to M'. We obtain these two ingredients via two different computational approaches.

A. Free energy landscape

For various values of L and B and various temperatures we make histograms of the distribution of the magnetization $M=\Sigma_i \sigma_i$ and the energy. Since the probability that a state with energy E occurs at an inverse temperature β is proportional to the Boltzmann weight $\exp(-\beta E)$, a histogram made at a certain temperature provides information about the probability distribution at nearby temperatures as well. We use the multiple histogram method [7] to combine the information from simulations at various temperatures. In this way, histograms for the magnetization over a wide range of temperatures can be obtained. As defined above, the free energy $F(M)$ is related to the probability that a certain magnetization M occurs by $P_{eq}(M)=e^{-\beta F(M)}$. The method of determining free energies of configurations constrained to some value of a coordinate along a pathway through phase space has been used extensively, for instance by Auer and Frenkel [8]. In Fig. 2 the free energy as a function of the magnetization per spin $m=M/N$ is plotted at two different temperatures and three different values of L/B.

In order to compare these results with theory we note that the probability $P_{eq}(0)$ of finding the system in a state with $M=0$ can be obtained from Eq. (4.23) of chapter V of Ref. [9] as follows. First note that this equation gives the following approximation for the partition function of a periodic antiferromagnetic system with one phase boundary [10],

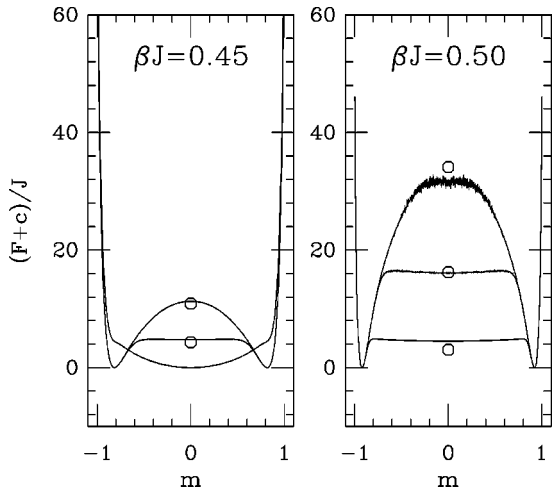

FIG. 2. Free energy (in units of J) as a function of magnetization at inverse temperatures $\beta J=0.45$ and $\beta J=0.50$. The number of spins is kept constant at 1024. The upper curves represent the 32×32 system, the middle curves represent the 16×64 system, and the lower curves represent the 8×128 system. The free energies at $M=0$ corresponding to Eq. (10) are also indicated. A constant c is added to the free energy curves, such that the minimal value of $F(M)+c$ is zero in all cases.

which is equivalent to a ferromagnetic system with an antiperiodic boundary:

$$Z_1=\frac{Z_0}{2}\sum_{k=1}^{2L}\left(\frac{A(k)-\sqrt{A^2(k)-c^2}}{A(k)+\sqrt{A^2(k)-c^2}}\right)^{B/2}, \tag{9}$$

where

$$A(k)=(1+z^2)^2-2z(1-z^2)\cos\frac{\pi k}{L},$$

$$c=2z(1-z^2),$$

$$z=\tanh\beta J,$$

and Z_0 the partition function for a homogeneous system (cf. Eq. (4.20) of Ref. [9]). Neglecting the possible interaction between two phase boundaries (or interfaces) we conclude that the partition function Z_2 for a system with two interfaces is given by $Z_2/Z_0=(1/2)(Z_1/Z_0)^2$. The factor 1/2 arises because otherwise we would count each configuration twice: interchanging the locations of the two interfaces does not give a different configuration. If we leave the positions of the two interfaces completely free, the magnetization is distributed almost uniformly over all possible even values between $-M_0$ and M_0. Therefore, fixing M to 0 leads to a reduction of the partition function by a factor of M_0. Thus we arrive at the following result for $P_{eq}(0)$:

$$P_{eq}(0)=\frac{Z_2}{M_0Z_0}=\frac{1}{8M_0}\left[\sum_{k=1}^{2L}\left(\frac{A(k)-\sqrt{A^2(k)-c^2}}{A(k)+\sqrt{A^2(k)-c^2}}\right)^{B/2}\right]^2. \tag{10}$$

For square systems this result has to be modified, because there are two ways to make a strip with opposite magnetization: the interfaces can lie in the horizontal as well as in the vertical direction. This gives an additional factor 2 in the equation for $P_{eq}(0)$.

B. Interface diffusion coefficient

The second ingredient for the theoretical framework in Sec. III consists of the transition rates $\Gamma_{M',M}$ from magnetization M to M'. As discussed there, we are actually mostly interested in the contribution to the transition rates that arises from the diffusion parallel to the longer periodic direction of interfaces that span the shorter one. To estimate this diffusion coefficient numerically, we study systems with antiperiodic boundary conditions: the spins in two neighboring sites $i<N-1$ and $j=i+1$, or in $i<N-B$ and $j=i+B$ are aligned if $\sigma_i=\sigma_j$, whereas the spins in two neighboring sites $i=N-1$ and $j=0$, or in $i\geqslant N-B$ and $j=i+B-N$, are aligned if $\sigma_i=-\sigma_j$.

The interface location $x(0)$ is initially defined as the magnetization $M(0)$. As long as $M\in[-0.8N,0.8N]$, steps Δx in the interface location are equal to changes ΔM in the magnetization, i.e., $x(t+\Delta t)-x(t)=M(t+\Delta t)-M(t)$. Once the interface gets close to the antiperiodic boundary, the magnetization does not uniquely determine the interface location. As soon as M is no longer in the interval $[-0.8N,0.8N]$, we shift the antiperiodic boundary away from the interface over half the system size (which will bring the magnetization back in this range) and then continue.

In practice, we achieve this by switching from monitoring M to monitoring $M'=\Sigma_{i=0}^{N/2-1}\sigma_i-\Sigma_{i=N/2}^{N-1}\sigma_i$, and $|x(t+\Delta t)-x(t)|=|M'(t+\Delta t)-M'(t)|$. The sign of the steps in $x(t)$ depends on the location of the interface: in the lower half this sign will be unchanged, whereas in the upper half it will be reversed. As soon as M' leaves the interval $[-0.8N,0.8N]$ we switch back to measuring steps in the original magnetization M. Also here, the sign of the steps in $x(t)$ depends on the location of the interface. Note that x is not confined to the interval $[-N,N]$. The diffusion coefficient D is then obtained from the time-dependent interface location $x(t)$ as

$$D=\lim_{t\to\infty}\left[\frac{\langle(x(t)-x(0))^2\rangle}{2t}\right]. \tag{11}$$

We expect that the interface diffusion coefficient is independent of L, and that it grows linearly with B since the number of sites where a spin flip moves the interface grows linearly with its width; however, for small B corrections arise due to the periodicity (or helicity) of the boundaries. Consequently, we expect

$$D(B,L,\beta J)=g(\beta J)B+c. \tag{12}$$

For temperatures close to T_c and small B, the system might occasionally contain more than a single interface. In that case, Eq. (11) would overestimate the diffusion coefficient of an interface. Since the additional free energy cost of interfaces increases linearly with B, this unwanted contribu-

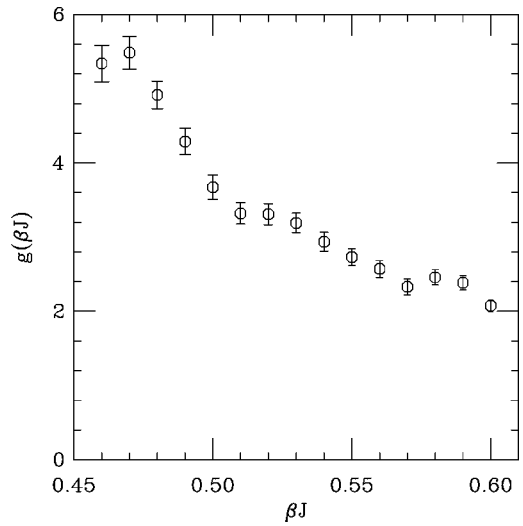

FIG. 3. Monte Carlo measurements of the diffusion coefficient per interface length $g(\beta J)$, as a function of inverse temperature βJ.

tion to D decreases exponentially with B. Taking this into account, our approach is to measure for various values of βJ, B, and L the diffusion coefficient D via Eq. (11). Next we determine the function $g(\beta J)$ in Eq. (12); the results are plotted in Fig. 3. Indeed we find that for increasing B and at temperatures not too close to T_c the diffusion coefficient rapidly becomes independent of L within the range of L values we considered. In our theoretical framework we then use an approximation for the jump rates

$$\min[\Gamma_{M,M+2},\Gamma_{M+2,M}]=\frac{g(\beta J)B}{2}. \tag{13}$$

This may be understood from the observations that on one hand one has $D=4\Gamma$, because the jumps in magnetization go by units of 2, on the other hand D satisfies Eq. (12) with B replaced by $2B$ because there are two interfaces. The above equation, in combination with Eq. (4) and the free energy as a function of magnetization, specifies all the transition rates. Using Eq. (8) we can now predict the magnetization reversal times. The results are shown in Table I.

C. Magnetization reversal times

We measure the magnetization every N attempted spin flips. We look for events, where the magnetization crosses from positive (more than half the spins up) to negative or vice versa between two consecutive measurements.

We make histograms of the times between two occurrences of magnetization reversal events. The histogram obtained in a system containing 16×64 spins, at the temperature corresponding to $\beta J=0.45$, is shown in Fig. 4. For comparison we also show a histogram of the times measured between the first time the system reaches a free energy minimum, and the first time after this it reaches the other minimum. We will come back to this in our discussion. The figure shows that at long times the decay function $f(t)$ behaves as $f(t)\sim\exp(-t/\tau)$. Here, we focus on the long-time behavior,

TABLE I. Estimated values for the magnetization reversal times.

βJ	32×32	16×64	16×32
0.46	1.66×10^{5}	1.74×10^{4}	1.19×10^{4}
0.47	1.12×10^{6}	4.21×10^{4}	3.15×10^{4}
0.48	8.88×10^{6}	1.25×10^{5}	9.96×10^{4}
0.49	7.38×10^{7}	3.97×10^{5}	3.31×10^{5}
0.50	6.49×10^{8}	1.31×10^{6}	1.12×10^{6}
0.51	5.83×10^{9}	4.19×10^{6}	3.61×10^{6}
0.52	5.31×10^{10}	1.23×10^{7}	1.05×10^{7}
0.53	5.77×10^{11}	3.78×10^{7}	3.11×10^{7}
0.54	7.69×10^{12}	1.23×10^{8}	9.60×10^{7}
βJ	16×16	8×64	8×32
0.46	4.43×10^{3}	2.76×10^{3}	1.24×10^{3}
0.47	1.06×10^{4}	3.26×10^{3}	1.73×10^{3}
0.48	3.09×10^{4}	4.72×10^{3}	2.88×10^{3}
0.49	9.56×10^{4}	7.45×10^{3}	5.11×10^{3}
0.50	3.09×10^{5}	1.26×10^{4}	9.47×10^{3}
0.51	9.60×10^{5}	2.12×10^{4}	1.69×10^{4}
0.52	2.73×10^{6}	3.32×10^{4}	2.77×10^{4}
0.53	8.06×10^{6}	5.50×10^{4}	4.71×10^{4}
0.54	2.50×10^{7}	9.69×10^{4}	8.43×10^{4}
0.55	7.64×10^{7}	1.70×10^{5}	1.49×10^{5}
0.56	2.30×10^{8}	2.96×10^{5}	2.61×10^{5}
0.57	7.20×10^{8}	5.38×10^{5}	4.75×10^{5}
0.58	1.92×10^{9}	8.37×10^{5}	7.39×10^{5}
0.59	5.54×10^{9}	1.42×10^{6}	1.25×10^{6}
0.60	1.77×10^{10}	2.66×10^{6}	2.34×10^{6}

and are specifically interested in the escape time τ. We obtain this quantity via a fitting procedure, in which we ignore the data up to a time t_0, chosen such that $f(t)$ shows exponential time behavior for $t>t_0$. Then we determine the time

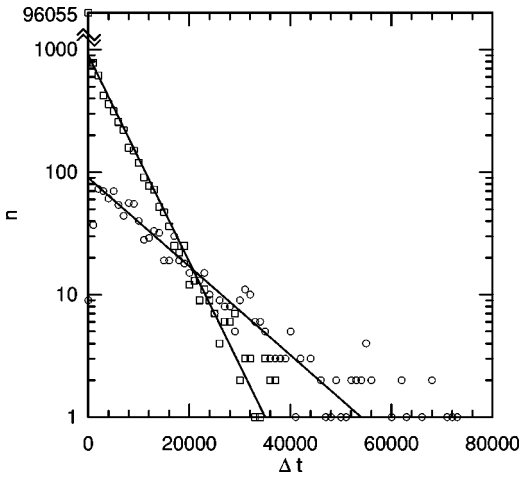

FIG. 4. Histogram of the times between zero crossings of the magnetization (squares), and the times between first occurrence of a free energy minimum (circles) in the 16×64 Ising model at $\beta J=0.45$. The solid lines depict the fit to the data, obtained as described in the text.

TABLE II. Directly measured values for the magnetization reversal times.

βJ	32×32	16×64	16×32
0.46	$2.09(6)\times10^5$	$1.52(3)\times10^4$	$1.37(1)\times10^4$
0.47	$2.02(6)\times10^6$	$5.14(5)\times10^4$	$4.18(4)\times10^4$
0.48	$1.97(6)\times10^7$	$1.68(1)\times10^5$	$1.32(1)\times10^5$
0.49		$5.20(5)\times10^5$	$4.26(6)\times10^5$
0.50		$1.62(5)\times10^6$	$1.33(2)\times10^6$
0.51		$5.2(1)\times10^6$	$4.28(6)\times10^6$
0.52		$1.59(5)\times10^7$	$1.32(3)\times10^7$
0.53		$4.5(2)\times10^7$	$4.0(1)\times10^7$
0.54		$1.40(6)\times10^8$	$1.13(4)\times10^8$
	16×16	8×64	8×32
0.46	$6.83(7)\times10^3$	$1.21(1)\times10^3$	$1.23(1)\times10^3$
0.47	$1.81(2)\times10^4$	$2.10(2)\times10^3$	$2.08(2)\times10^3$
0.48	$4.8(2)\times10^4$	$3.75(3)\times10^3$	$3.61(4)\times10^3$
0.49	$1.35(4)\times10^5$	$6.70(7)\times10^3$	$6.30(6)\times10^3$
0.50	$4.45(4)\times10^5$	$1.20(1)\times10^4$	$1.11(1)\times10^4$
0.51	$1.26(1)\times10^6$	$2.07(2)\times10^4$	$1.99(2)\times10^4$
0.52	$3.82(5)\times10^6$	$3.66(3)\times10^4$	$3.37(3)\times10^4$
0.53	$1.13(2)\times10^7$	$6.36(6)\times10^4$	$5.87(5)\times10^4$
0.54	$2.97(6)\times10^7$	$1.09(1)\times10^5$	$1.04(2)\times10^5$
0.55	$9.7(3)\times10^7$	$1.95(3)\times10^5$	$1.68(3)\times10^5$
0.56	$1.9(2)\times10^8$	$3.26(6)\times10^5$	$3.05(9)\times10^5$
0.57		$5.40(8)\times10^5$	$4.5(1)\times10^5$
0.58		$9.2(2)\times10^5$	$8.3(2)\times10^5$
0.59		$1.61(2)\times10^6$	$1.41(3)\times10^6$
0.60		$2.67(5)\times10^6$	$2.64(8)\times10^6$

t' at which half of the remaining events have taken place. The escape time τ is then obtained from $\tau=(t'-t_0)/\ln(2)$. Instead we could have made a linear fit of all the data points beyond t_0, but this makes no significant difference.

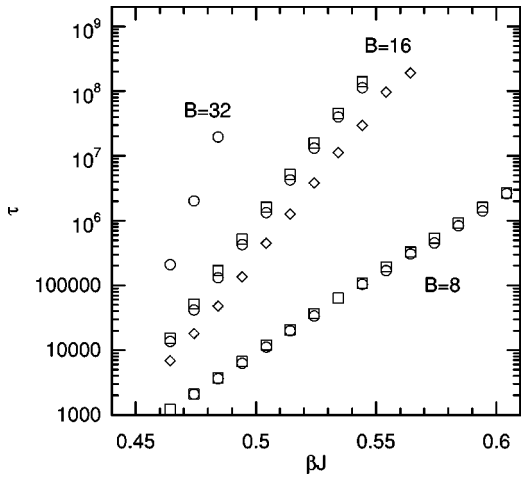

FIG. 5. Magnetization reversal times τ as a function of inverse temperature βJ, for various system sizes. The diamonds represent systems with $L=16$, the circles represent systems with $L=32$, and the squares represent systems with $L=64$.

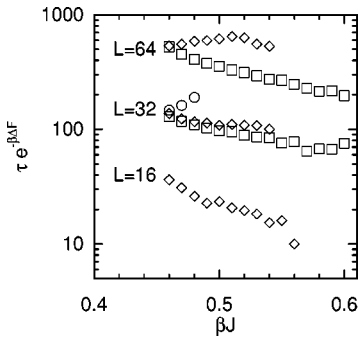

FIG. 6. Ratio of the magnetization reversal times τ and $\exp(\beta\Delta F)$, as a function of inverse temperature βJ, for various system sizes. The squares represent systems with $B=8$, the diamonds represent systems with $B=16$, and the circles represent systems with $B=32$.

The resulting reversal times, for several system sizes and inverse temperatures, are presented in Table II and plotted in Fig. 5. One sees by comparing the results of Tables I and II that in most cases the two agree within 20% for temperatures not too close to the critical temperature.

A commonly used first approximation to the description of the time scales of activated processes is Arrhenius' law, which states that the typical time scale τ increases exponentially with the height of the (free) energy barrier $\Delta F \equiv F(M=0)-F(M=M_0)$, with a prefactor f that depends in a mild way on temperature and system size,

$$\tau = f(\beta,B,L)\exp(\beta\Delta F). \tag{14}$$

If we straightforwardly use the free energy $F(M)$ as defined before we can obtain the heights of the free-energy barriers directly from the histograms of the magnetization distribution. To check the accuracy of this, we have plotted in Fig. 6 the ratio of τ and $\exp(\beta\Delta F)$ as a function of inverse temperature βJ, for various system sizes. Clearly, if the prefactor f is assumed to be constant, this simple approximation fails to even predict the magnetization reversal times within an order of magnitude.

A little thought reveals that, in the present case, this way of determining the free energy barrier is not entirely satisfactory. The reason is that for magnetization values around $M=M_0$ the free energy increases with system size because the range of values through which M typically fluctuates, increases as the square root of system size. As a consequence the probability of finding any specific M-value decreases. Around $M=0$ on the other hand, no similar effect occurs, due to the wide plateau of the free energy as function of M. As a result of this the decrease of probability of finding a given magnetization value for given relative position of the two interfaces is precisely compensated by the probabilities of finding this same magnetization value at different relative positions. Therefore, it makes more sense in this case to define the Arrhenius factor in an alternative way as $\exp[\beta F(M=0)]$. With this definition, where again $\beta F(M) = -\ln[P_{eq}(M)]$, it may be interpreted indeed as the equilibrium probability of finding two interfaces dividing the system into equal areas. But please notice that if, instead of a

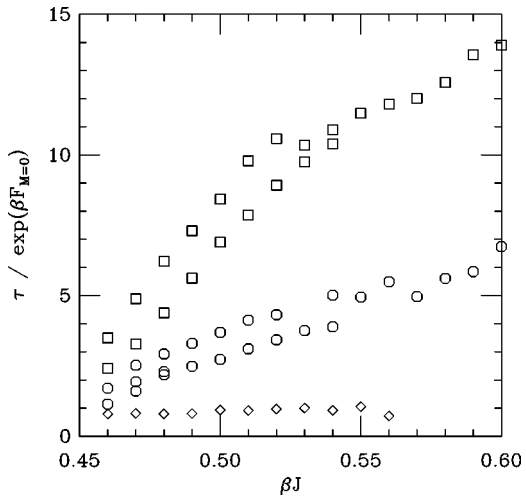

FIG. 7. Ratio of the magnetization reversal times τ and $\exp[\beta F(0)] \equiv P_{eq}(M=0)^{-1}$, as a function of inverse temperature βJ, for various system sizes. The squares represent systems with $L=64$, the circles represent systems with $L=32$, and the diamonds represent systems with $L=16$.

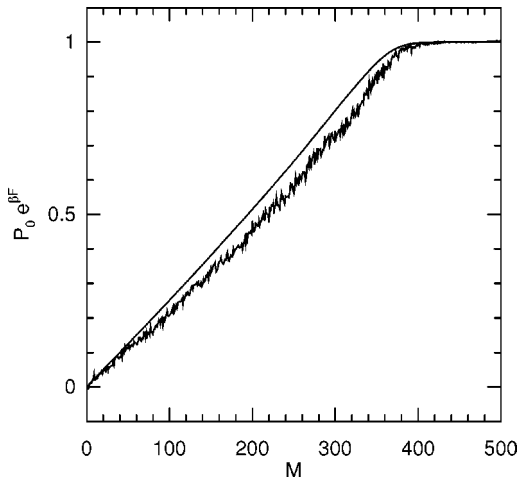

FIG. 8. The most slowly decaying eigenmode $P_0(M)$ divided by the equilibrium distribution $\exp[-\beta F(M)]$ for the 16×64 system at $\beta J=0.5$, obtained in two different ways as described in the text. Since this function is antisymmetric in M, the left-hand side of the figure ($M<0$) has been left out for clarity.

plateau, the free energy has a maximum of a width small compared to the range of magnetization fluctuations, the first definition of the Arrhenius factor is to be preferred.

With the second definition the expression for the decay time in terms of the Arrhenius factor becomes

$$\tau = f'(\beta,B,L)\exp(\beta F(M=0)), \tag{15}$$

in which again one hopes that the prefactor f' depends on temperature and system dimensions only in a mild way. On the basis of Eqs. (8) and (13) we may conclude that for large systems f' should simply be proportional to L and independent of B.

Figure 7 shows f' as a function of inverse temperature for several system sizes. For $L=32$ and 64 both the approximate independence of B and the proportionality to L are quite well confirmed, especially if one takes into account that the plateau widths for these system sizes are notably less than L (see Fig. 2). For $L=16$ the plateau becomes so narrow that the above predictions do not apply.

D. Most slowly decaying mode

To obtain an estimate for the magnetization reversal times, we first estimated the most slowly decaying mode in Eq. (7). Besides comparing the magnetization reversal times, we can also obtain the most slowly decaying eigenmode $P_0(M)$ directly from our Monte Carlo simulations by measuring the probability difference between the occurrence of a certain magnetization M and the occurrence of the opposite magnetization $-M$, averaged over a time scale comparable to the magnetization reversal time τ. Since P_0 decays much slower than the other antisymmetric (in M) modes, it will give the dominant contribution to this probability difference. Figure 8 compares the most slowly decaying eigenmode as obtained with Eq. (7) with the direct Monte Carlo measurements, for the 16×64 system at $\beta J=0.5$.

V. DISCUSSION

Our simulations confirm the global picture we sketched for the process of magnetization reversals in the Ising model with stochastic dynamics: a large cluster of opposite magnetization, originating through a fluctuation develops into a pair of interfaces. These interfaces diffuse around the system and annihilate, leaving the system in the oppositely magnetized phase. Quantitatively this process may be described to a good approximation as a diffusion process in a one-dimensional space with a coordinate describing the total magnetization in the system.

A few remarks should be made here.

(i) First of all it may seem remarkable that in almost all cases our theoretical prediction gives a shorter reversal time than the simulations. Since the theory neglects processes that enhance the reversal frequency, such as the formation of more than two simultaneous interfaces and spurious passages of $M=0$ (see below), one might expect an overestimate of the reversal time rather than an underestimate. The explanation of the latter comes primarily from that part of the process in which a growing cluster of opposite magnetization transforms into a band around the cylinder. As the cluster will at first be typically circular in shape (if the temperature is not too low) it has to deform into a more elliptical shape, with a longer interface than the band, before the latter can be formed. In Fig. 2 the signs of this are very clear in the form of little shoulders on the sides of the plateaus in the free energies. The transition rates $\Gamma_{M',M}$ for the formation of these elliptical shapes will not be proportional to B but much smaller, since this growth mainly occurs along the short sides of the cluster. The contributions from these terms in the denominator of Eq. (8) are therefore larger than estimated. Numerically they are important as long as the plateau in the free energy is not too wide. This will give rise to a notable decrease of the reversal frequencies from our estimated values. Correcting for this in the theoretical expression would require better estimates of $\Gamma_{M',M}$ in the free energy shoulders,

which seem fairly complicated to obtain. Also the growth rates in the magnetization regions beyond the shoulders, where the growing clusters are even smaller, are overestimated by Eq. (13), but these are weighted less as the free energies there are smaller.

(ii) The above considerations clearly reveal the possibility that the coordinate parametrizing the ''reaction path'' (here the magnetization) changes nonmonotonically along this reaction path; one could imagine that the growing cluster, before turning into a strip, typically decreases in size for a while. In reality this does not seem to happen, but if this were the case, parts of the reaction path with different cluster shape but equal magnetization would be lumped together, and the diffusion process along the cluster size coordinate would no longer correspond to the actual path taken by the cluster. Obviously in such a case the reaction coordinate has to be redefined in such a way that the new coordinate is monotonic along the reaction path indeed. But in complicated situations it may not always be clear what is a proper choice for such a coordinate.

(iii) As a consequence of magnetization fluctuations in the bulk, passages of $M=0$ will be registered typically already a short while before the area between the interfaces reaches the value $LB/2$ corresponding to an equal division of the system between areas of positive and negative magnetization. The reason is that the typical time scale for fluctuations of the bulk magnetization is much shorter than that for interface diffusion, so for each location of the interfaces the whole range of accessible magnetization values typically will be scanned. Now in most cases this just will give rise to a negligible shift of the time at which the situation of equal areas (this is the physically relevant criterion) is reached, but occasionally it may happen that $M=0$ occurs, but the system returns to the pure state it came from without ever reaching equal areas. To check the importance of these events we may compare the average first passage time from $-M_0$ to M_0 to that from $\pm M_0$ to $M=0$. If the effect of magnetization fluctuations is negligible the ratio of these should be 2, otherwise it ought to be larger. Note that for the systems considered here the effect of magnetization fluctuations on the first passage time from $-M_0$ to M_0 is much smaller than that on the first passage time from $-M_0$ to $M=0$, because the probability of returning to $-M_0$ without reaching the pure state of positive magnetization, once $M=M_0$ has been reached, is extremely small. We have measured this ratio for several system sizes and temperatures, excluding those cases where the occurrence of multiple interfaces is likely, and found that the mean value is 1.90, with a standard deviation of 0.15.

(iv) It is of interest to investigate how the reversal times depend on the system size parameters. From Eq. (8) we may conclude that for long systems (but not so long that multiple interface pairs will occur frequently) the reversal time will become independent of the system length L. For this one should notice first of all that for M values on the plateau $\exp[\beta F(M)]$ is proportional to $1/L$, because the number of ways a pair of interfaces may be placed such that the average magnetization equals M, is proportional to L. On the other hand the summation over M, which is dominated by M values on the plateau, gives rise to a factor close to L. Hence to first approximation the reversal frequency ν is independent of L. Remarkably this independence of L in fact is observed even better by the numerical results than by the theoretical estimates.

In Sec. IV C it was noted already that the product f' of the reversal frequency and the Arrhenius factor $\exp(-\beta F(0))$ depends on L and βJ, but is approximately independent of the system width B. Notice that square systems may be included in this comparison without problem, as the extra factor of 2 due to the two possible orientations of the interfaces, is properly accounted for in the Arrhenius factor.

(v) We already indicated repeatedly that our theory may be applied only if the probability of having more than two interfaces around the cylinder may be neglected compared to the probability of having just two such interfaces. For this to be the case one has to require $Z_1/Z_0 \ll 1$. For large enough systems this condition may be rewritten as $L \ll \exp(\beta\sigma B)$, with σ the surface tension of the interface. For large systems violation of this condition requires extreme aspect ratios, so under normal conditions it will be satisfied, unless the temperature is very close to the critical one, at which the surface tension vanishes.

We are presently applying the methods described here to a study of nucleation rates in metastable states. We hope to report on this before long.

[1] P.A. Rikvold, G. Brown, S.J. Mitchell, and M.A. Novotny, in *Nanostructured Magnetic Materials and their Applications*, edited by D. Shi, B. Aktas, L. Pust, and F. Mikailov, Springer Lecture Notes in Physics, Vol. 593 (Springer, Berlin, 2002), p. 164.

[2] A. Misra and B.K. Chakrabarti, Europhys. Lett. **52**, 311 (2000).

[3] M.P. Nightingale and H.W.J. Blöte, Phys. Rev. B **62**, 1089 (2000).

[4] M.E.J. Newman and G.T. Barkema, *Monte Carlo Methods in Statistical Physics* (Oxford University Press, Oxford, 1999).

[5] N. Metropolis, A.W. Rosenbluth, M.N. Rosenbluth, A.H. Teller, and E. Teller, J. Chem. Phys. **21**, 1087 (1953).

[6] P. Hänggi, P. Talkner, and M. Borkovec, Rev. Mod. Phys. **62**, 251 (1990).

[7] A.M. Ferrenberg and R.H. Swendsen, Phys. Rev. Lett. **63**, 1195 (1989).

[8] S. Auer and D. Frenkel, Nature (London) **409**, 1020 (2001).

[9] B.M. McCoy and T.T. Wu, *The Two-Dimensional Ising Model* (Harvard University Press, Cambridge, 1973).

[10] McCoy and Wu give the partition function for a system with nonhelical boundary conditions, whereas we have used helical boundary conditions. This should only make a difference at very low temperatures.